Journal of Sound and Vibration ∎ (∎∎∎∎) ∎∎∎–∎∎∎

Contents lists available at ScienceDirect

Journal of Sound and Vibration

journal homepage: www.elsevier.com/locate/jsvi

Feedback control unit with an inerter proof-mass electrodynamic actuator

Michele Zilletti

Institute of Sound and Vibration Research, University of Southampton, Southampton SO17 1BJ, UK

ARTICLE INFO

Article history:
Received 21 September 2015
Received in revised form
15 January 2016
Accepted 19 January 2016
Handling Editor: J. Lam

Keywords:
Velocity feedback
Inerter
Inertial actuator
Proof-mass actuator

ABSTRACT

In this study the use of an inerter is considered for active vibration control of a structure excited by white noise. The structure is modelled as a single degree of freedom system and the control system consists of a vibration absorber with a mass suspended on a spring, a damper and an inerter. The absorber is equipped with a reactive force transducer in parallel with the passive suspension which is driven with a signal proportional to the velocity of the structure under control measured by an ideal collocated sensor. The effect of the inerter on the control stability and performance of the control system is investigated. It is shown that the effect of the inerter is to reduce the natural frequency of the inertial actuator, improving the stability of the feedback loop and thus its performance. The optimisation of the physical and control parameters of the control system such as the internal damping of the actuator, its natural frequency, its inertance and the feedback gain are considered such that either the kinetic energy of the host structure is minimised or the power dissipated by the control system is maximised.

1. Introduction

Passive tuned vibration absorbers were proposed by Farhm [1] in 1911 and have been widely used to control structural vibrations ever since. They normally consist of a mass suspended on an elastic mount, which can usually be modelled as a single degree of freedom system. When they are used to control the vibration of flexible structures subjected to broadband excitation their natural frequency and internal damping are tuned to reduce the structural response in a narrow frequency band around a structural resonance [2]. Many optimisation criteria of passive vibration absorbers have been proposed depending on the application and a vast literature can be found on this topic [2–11]. As summarised by Zilletti et al. [11] several criteria have been derived using lumped parameter models. One drawback of passive vibration absorbers is that they can only be tuned to one resonance frequency of the host structure at the time and very small reduction is achieved at other resonance frequencies. Therefore multi-degrees of freedom absorbers [12] or time variant one [13–15] have been proposed in order to widen the frequency band of operation of these devices. However the efficiency of passive and semi-active vibration absorbers increases with the mass ratio of the absorber to the system under control resulting in high added weight.

A considerable improvement can be achieved by using active vibration absorbers, which consist of a passive vibration absorber with a reactive force transducer in parallel with the suspension, which is driven to implement a feedback loop. An example of this device is the voice coil inertial actuator with an accelerometer sensor at its footprint commonly used in

E-mail address: m.zilletti@soton.ac.uk

http://dx.doi.org/10.1016/j.jsv.2016.01.035
0022-460X/

Please cite this article as: M. Zilletti, Feedback control unit with an inerter proof-mass electrodynamic actuator, *Journal of Sound and Vibration* (2016), http://dx.doi.org/10.1016/j.jsv.2016.01.035

vibration control applications [16]. The advantages of an active vibration absorber are its adaptability to parameters changes of the structure under control, which guarantees a better vibration control performance in a wider range of operating conditions compared with a passive one. Depending on the circumstances, active solutions may be cheaper and lighter than passive systems offering performances that no passive system can achieve, especially in controlling low frequency vibration. One way of driving these devices in order to damp the structural response of flexible structures subjected to broadband excitation is by using a velocity feedback loop [17–20]. In this case the controller acts as a sky-hook active damper in the frequency region above the resonance of the actuator, before higher order resonances interfere with their dynamics. This type of control system is only conditionally stable because of the 180° phase shift in the response of the actuator due to its resonance. In order to improve the stability of the controller and thus its performance, the natural frequency of the absorber has to be as low as possible compared to the natural frequency of the structure under control [21]. This may be achieved by using a low suspension stiffness which, however, may cause problems with the static deflection of the suspended mass due to gravity. This can be overcome with internal displacement feedback loops [22]. In a similar manner, internal velocity feedback loops can be used to increase the internal damping [23]. These methods require external power and particular care has to be taken in the practical implementation of the feedback loop to avoid instability phenomena. Another strategy to improve the stability of these devices is by using a compensator which electronically shifts the resonance frequency of the device at lower frequency with the drawback of increasing the feedback signal in the low frequency region which may result in a stroke/force saturation effect of the actuator [24].

In this paper the use of an inerter that lowers the fundamental resonance frequency of the actuator is investigated. The inerter is a mechanical device which produces a force proportional to the relative acceleration of its two terminals and was initially proposed by Smith [25]. The constant of proportionality is called inertance and is measured in kilogram. Since its invention inerters have been widely used and a vast literature can be found on their applications. Although a complete literature review on this topic is beyond the scope of this paper, it is instructive to consider few examples of inerters in vibration control applications. Inerters have been previously used in vibration absorbers with the aim of improving their performance in damping out the vibration of both linear [26] and nonlinear systems [27]. Also, vibration absorbers with tuneable inertance have been proposed which use a continuously variable transmission and gear ratio control system [28]. Inerters have been used to improve the performance of passive [29–31] and semi-active car suspensions [32]. In the case of semi-active suspensions the inertance is electronically synthetised with a state- feedback control system. Several applications of inerters can be found in different systems such as passive network synthesis [33–35], motorcycles steering system [36,37], train suspensions [38,39], civil engineering applications [40], and landing gear suspensions [41] with the aim of improving vibration control performance.

Chen et al. [42] have demonstrated that the natural frequency of a lumped parameter mechanical system with an inerter can always be reduced by increasing the inertance. This suggests that the use of an inerter in an active vibration absorber could be used to improve its control stability by lowering the resonance frequency of the device without softening the suspension.

In this paper the proposed vibration absorber that implements an ideal velocity feedback loop is used to control a single mode of a vibrating structure, modelled as a single degree of freedom system, which is subjected to white noise excitation. Throughout the paper, to better emphasise the advantages of the proposed control unit, the vibration control effect of the proposed device with the inerter is compared with the effect produced by a reference control unit without the inerter. It is demonstrated that the use of the inerter improves the control stability and thus provides a better control performance compare to the configuration without the inerter.

One important issue with such a control system is how the feedback gain is set to optimally control the vibration of the hosting structure. In an ideal system, the optimal feedback gain would be adjusted to minimise the kinetic energy of the structure under control. However this optimisation may be difficult to implement in practice because it would require velocity measurements in many points of the structure. Previous studies have shown that the maximisation of power absorbed by the controller, which can be easily estimated from the feedback signal, is equivalent to the minimisation of the kinetic energy of the structure under control subjected to a white noise excitation [43–45]. This paper extends this result to the case of the control unit with the inerter.

The organisation of the paper is as follow. In Section 2 the mathematical model of the primary system with the controller is derived providing the expressions for the frequency response functions. In Section 3 the stability of the control system is analytically assessed and the expressions for the kinetic energy of the system under control and the power absorbed by the controller are derived. In Section 4 numerical simulation results are presented and conclusions are drawn in Section 5.

2. Mathematical model

Typically when an inertial actuator is used to implement a velocity feedback loop to control the resonant response due to one mode of a flexible structure, a simplified lumped parameters model is considered. As shown in Fig. 1 it is assumed that the primary structure is composed by a modal mass m_1, a damper c_1 and a stiffness k_1 and is excited by a primary force f_p.

Classical inertial actuators are composed by a block mass m_2, mounted on a suspension of stiffness k_2 a damping c_2. In this study an inerter of inertance b_2, producing a force proportional to the relative acceleration between mass m_1 and m_2 has been added in parallel with a reactive force transducer. At frequencies above its fundamental resonance frequency, the

Please cite this article as: M. Zilletti, Feedback control unit with an inerter proof-mass electrodynamic actuator, *Journal of Sound and Vibration* (2016), http://dx.doi.org/10.1016/j.jsv.2016.01.035

inertial actuator produces a sky-hook active force f_a proportional to the absolute velocity of the modal mass m_1 via the control gain g.

The equation of motion of the system shown in Fig. 1 can be written in a matrix form as:

$$\mathbf{M}\ddot{\mathbf{x}}(t)+\mathbf{C}\dot{\mathbf{x}}(t)+\mathbf{K}\mathbf{x}(t)=\boldsymbol{f}(t) \tag{1}$$

where **M** is the mass matrix, **K** is the stiffness matrix and **C** is the damping matrix given by:

$$\mathbf{M}=\begin{bmatrix} m_1+b_2 & -b_2 \\ -b_2 & m_2+b_2 \end{bmatrix}, \mathbf{K}=\begin{bmatrix} k_1+k_2 & -k_2 \\ -k_2 & k_2 \end{bmatrix}, \mathbf{C}=\begin{bmatrix} c_1+c_2+g & -c_2 \\ -c_2-g & c_2 \end{bmatrix}, \tag{2}$$

$\mathbf{x}(t)=[x_1(t) \quad x_2(t)]^T$ is the column vector containing the displacements of the two masses x_1 and x_1 and $\mathbf{f}(t)=\begin{bmatrix} f_p(t) & 0 \end{bmatrix}^T$ is the column vector of the primary excitation. It is important to notice that due to the feedback loop the damping matrix **C** is non-symmetric. As it will be shown in the next section this implies that the control system is only conditionally stable.

Assuming the excitation to be harmonic for the time being and expressing the force and the steady-state response in exponential form, Eq. (1) becomes:

$$\mathbf{S}(\mathrm{j}\omega)\mathbf{x}(\mathrm{j}\omega)=\mathbf{f}(\mathrm{j}\omega) \tag{3}$$

where

$$\mathbf{S}(\mathrm{j}\omega)=-\omega^2\mathbf{M}+\mathrm{j}\omega\mathbf{C}+\mathbf{K} \tag{4}$$

is the dynamic stiffness matrix. The solution of Eq. (3) can be obtained as:

$$\mathbf{x}(\mathrm{j}\omega)=\mathbf{S}^{-1}(\mathrm{j}\omega)\mathbf{f}(\mathrm{j}\omega). \tag{5}$$

Integrating Eq. (5) to obtain the velocities yields:

$$\dot{\mathbf{x}}(\mathrm{j}\omega)=\mathbf{Y}(\mathrm{j}\omega)\mathbf{f}(\mathrm{j}\omega), \tag{6}$$

where $\dot{\mathbf{x}}(\mathrm{j}\omega)=\mathrm{j}\omega\mathbf{x}(\mathrm{j}\omega)$ and $\mathbf{Y}(\mathrm{j}\omega)=\mathrm{j}\omega\mathbf{S}^{-1}(\mathrm{j}\omega)$ is the mobility matrix. Using the expression of **M**, **K** and **C** of Eq. (2), the steady state complex response of the system can be expressed in terms of the input and transfer frequency response functions (FRF) as:

$$Y_{11}(\mathrm{j}\omega)=\frac{\dot{x}_1}{f_p}=$$

$$=\frac{\mathrm{j}k_2\omega-\mathrm{c}_2\omega^2-\mathrm{j}m_2\omega^3-\mathrm{j}b_2\omega^3}{k_1k_2+\mathrm{j}\mathrm{c}_2k_1\omega+\mathrm{j}\mathrm{c}_1k_2\omega-\mathrm{c}_1\mathrm{c}_2\omega^2-b_2k_1\omega^2-k_2m_1\omega^2-k_1m_2\omega^2-k_2m_2\omega^2-\mathrm{j}b_2c_1-\mathrm{j}\mathrm{c}_2m_1\omega^3-}$$

$$\mathrm{j}\mathrm{c}_1m_2\omega^3-\mathrm{j}\mathrm{c}_2m_2\omega^3+gm_2\omega^2+b_2m_1\omega^4+b_2m_2\omega^4+m_1m_2\omega^4 \tag{7}$$

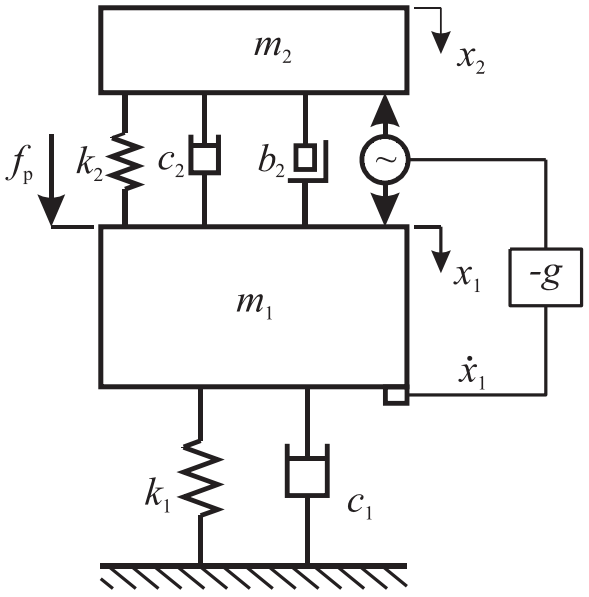

Fig. 1. Scheme of the SDOF system with a velocity feedback loop using an inertial actuator.

Please cite this article as: M. Zilletti, Feedback control unit with an inerter proof-mass electrodynamic actuator, *Journal of Sound and Vibration* (2016), http://dx.doi.org/10.1016/j.jsv.2016.01.035

$$Y_{21}(\mathrm{j}\omega)=\frac{\dot{x}_2}{f_p}=$$
$$=\frac{\mathrm{j}k_2\omega-\mathrm{c}_2\omega^2+g\omega^2-\mathrm{j}b_2\omega^3}{k_1k_2+\mathrm{j}\mathrm{c}_2k_1\omega+\mathrm{j}\mathrm{c}_1k_2\omega-\mathrm{c}_1\mathrm{c}_2\omega^2-b_2k_1\omega^2-k_2m_1\omega^2-k_1m_2\omega^2-k_2m_2\omega^2-\mathrm{j}b_2c_1-\mathrm{j}\mathrm{c}_2m_1\omega^3-}$$

$$\mathrm{j}\mathrm{c}_1m_2\omega^3-\mathrm{j}\mathrm{c}_2m_2\omega^3+gm_2\omega^2+b_2m_1\omega^4+b_2m_2\omega^4+m_1m_2\omega^4 \tag{8}$$

where $\dot{x}_1$ and $\dot{x}_2$ are the complex frequency dependent velocities of masses m_1 and m_2 respectively. The two FRFs can be expressed in non-dimensional form as follows:

$$\Gamma(\mathrm{j}\lambda)=\frac{B_0+(\mathrm{j}\lambda)B_1+(\mathrm{j}\lambda)^2B_2+(\mathrm{j}\lambda)^3B_3}{A_0+(\mathrm{j}\lambda)A_1+(\mathrm{j}\lambda)^2A_2+(\mathrm{j}\lambda)^3A_3+(\mathrm{j}\lambda)^4A_4} \tag{9}$$

$$\Theta(\mathrm{j}\omega)=\frac{C_0+(\mathrm{j}\lambda)C_1+(\mathrm{j}\lambda)^2C_2+(\mathrm{j}\lambda)^3C_3}{A_0+(\mathrm{j}\lambda)A_1+(\mathrm{j}\lambda)^2A_2+(\mathrm{j}\lambda)^3A_3+(\mathrm{j}\lambda)^4A_4}, \tag{10}$$

where the coefficients A_{0-4}, B_{0-3} and C_{0-3} are given by:

$$\begin{array}{lll}
A_0=\nu^2 & B_0=0 & C_0=0\\
A_1=2\zeta_2\nu+2\zeta_1\nu^2 & B_1=\nu^2 & C_1=\nu^2\\
A_2=\nu^2+1+\mu\nu^2+4\zeta_1\zeta_2\nu+\delta & B_2=2\zeta_2\nu & C_2=2\zeta_2\nu+4\alpha\zeta_2\nu\\
A_3=2\zeta_2\nu+2\zeta_2\mu\nu+2\zeta_1+4\alpha\nu\zeta_2\mu+2\zeta_1\delta & B_3=1+\delta & C_3=\delta\\
A_4=1+\delta+\delta\mu &&
\end{array}$$

The seven non-dimensional parameters in Eqs. (9) and (10) are defined by:

$$\begin{aligned}
\mu&=m_2/m_1\\
\nu&=\omega_2/\omega_1\\
\lambda&=\omega/\omega_1\\
\zeta_1&=c_1/(2m_1\omega_1)\\
\zeta_2&=c_2/(2m_2\omega_2)\\
\alpha&=g/(2c_2)\\
\delta&=b_2/m_2
\end{aligned} \tag{11}$$

where μ is the mass ratio, ν is the frequency ratio, λ is the normalised driving frequency, ζ_1 and ζ_2 are the primary and secondary damping ratios respectively, α is the normalised velocity control feedback gain and δ is the normalised inertance. The natural frequency of the primary system, ω_1, and the natural frequency of the inertial actuator, ω_2, are defined as:

$$\begin{aligned}
\omega_1&=\sqrt{k_1/m_1},\\
\omega_2&=\sqrt{k_2/m_2}.
\end{aligned} \tag{12}$$

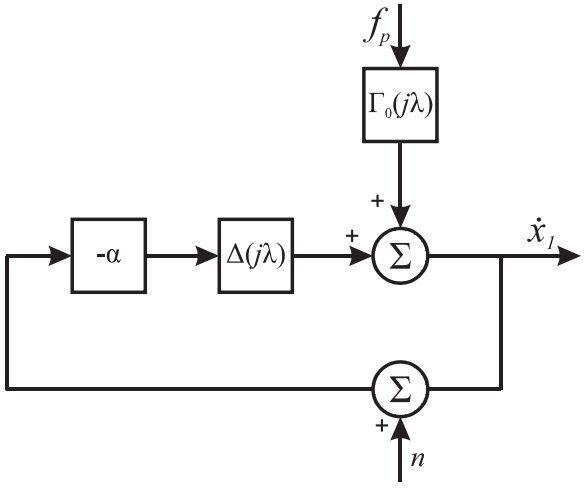

Fig. 2. Block diagram of the control system with measurement noise n.

3. Stability and performance

In this section the stability of the control system is analytically assessed and the expressions for the kinetic energy of the primary system and the power absorbed by the controller are derived.

3.1. Stability of the controller

It is important to notice that due to the resonance of the inertial actuator the velocity loop is only conditionally stable thus the control gain cannot exceed the value that leads the system to instability. Fig. 2 shows the block diagram of the control system where $\Delta(\mathrm{j}\lambda)$ is the open loop frequency response function given by:

$$\Delta(\mathrm{j}\lambda) = \Theta_0(\mathrm{j}\lambda) - \Gamma_0(\mathrm{j}\lambda). \tag{13}$$

where $\Gamma_0(\mathrm{j}\lambda)$ and $\Theta_0(\mathrm{j}\lambda)$ are obtained from Eqs. (9) and (10) by setting α to zero.

The stability of the controller can be assessed from the open loop frequency response function applying the Routh's stability criterion. The characteristic equation of the control system is given by the denominator of Eq. (13) and the related Routh's coefficients are listed in Table 1.

The coefficients of the characteristic equation are all positive and so is the coefficient h_1. To guarantee the stability of the system the numerator of coefficient h_2 has to be greater than zero and thus the following condition has to be satisfied:

$$S_2\alpha^2 + S_1\alpha + S_0 > 0 \tag{14}$$

where S_2, S_1 and S_0 are given by:

$$\begin{aligned} S_2 &= 2\nu(\mu\nu^3\zeta_1^2 + \zeta_1\left((1+\delta)^2 - 2(1+\delta+\delta\mu)\nu^2 + (1+\mu)^2\nu^4 + 4(1+\delta)\nu^2\zeta_1^2\right)\zeta_2 + \nu(\mu + 4(1+\delta \\ &\quad + (1+\mu)\nu^2)\zeta_1^2)\zeta_2^2 + 4(1+\mu)\nu^2\zeta_1\zeta_2^3) \\ S_1 &= 4\mu\nu^2\zeta_2\left((1+\delta-(1+\mu)\nu^2)\zeta_2 + 4\nu^2\zeta_1^2\zeta_2 + \nu\zeta_1\left(-1-\delta+(1+\mu)\nu^2+4\zeta_2^2\right)\right) \\ S_0 &= -8\mu^2\nu^4\zeta_2^2 \end{aligned} \tag{15}$$

Table 1
Routh's coefficients chart.

A_4	A_2	A_0
A_3	A_1	
$h_1 = \frac{A_3A_2 - A_4A_1}{A_3}$	A_0	
$h_2 = \frac{h_1A_1 - A_3A_0}{h_1}$		
A_0		

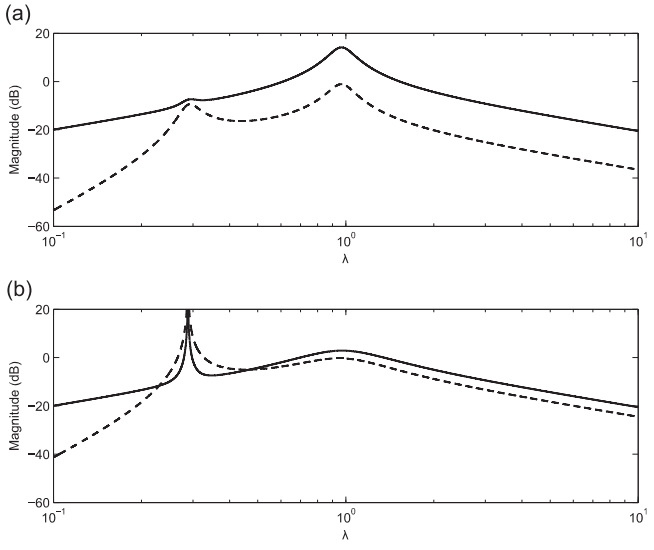

Fig. 3. Magnitude of the sensitivity (solid line) and the complementary sensitivity (dashed line) functions for $\alpha_{\max}/4$ (plot (a)) and for the control gain approaching the maximum stable gain $\alpha_{\max}$ (plot (b)).

Please cite this article as: M. Zilletti, Feedback control unit with an inerter proof-mass electrodynamic actuator, *Journal of Sound and Vibration* (2016), http://dx.doi.org/10.1016/j.jsv.2016.01.035

The block diagram shown in Fig. 2 also includes the signal n which represents measurement errors or noise on the feedback signal. The block diagram reduction indicates that the closed-loop output is given by:

$$\dot{x}_1 = \frac{\Gamma_0(\mathrm{j}\lambda)}{1+g\Delta(\mathrm{j}\lambda)} f_p - \frac{\Gamma_0(\mathrm{j}\lambda)\alpha\Delta(\mathrm{j}\lambda)}{1+\alpha\Delta(\mathrm{j}\lambda)} n = S(\mathrm{j}\lambda) f_p - T(\mathrm{j}\lambda) n \tag{16}$$

where the transfer functions $S(\mathrm{j}\lambda)$ and $T(\mathrm{j}\lambda)$ are usually defined as sensitivity and complementary sensitivity function respectively. Fig. 3 shows the magnitude of $S(\mathrm{j}\lambda)$ (solid line) and $T(\mathrm{j}\lambda)$ (dashed line) functions for low values of control gain (plot (a)) and for the control gain approaching the maximum stable gain (plot (b)).

Plot (a) shows that the magnitude of $T(\mathrm{j}\lambda)$ is lower than $S(\mathrm{j}\lambda)$ thus the control system has a good feedback noise rejection. However as shown in plot (b), when the control gain approaches the maximum stable gain the magnitude of $T(\mathrm{j}\lambda)$ gets larger than $S(\mathrm{j}\lambda)$ in the frequency region around the natural frequency of the control unit. This brief analysis shows that particular care must be taken in reducing the noise in the feedback signal since an excessive noise level may limit the control gain that can be achieved in practice and thus degrade the performance of the system.

3.2. Energy and power formulation

The performance of the controller discussed in the next section is assessed in terms of the reduction of the kinetic energy of the system under control when excited by a broadband white noise force. The kinetic energy of the primary mass per unit excitation force with a uniform power spectral density (PSD) $S_f(\omega)$ measured in N^2 s/rad is given by:

$$E_k = \frac{m_1 E\left[|\dot{x}_1(t)|^2\right]}{2S_f\omega_1/k_1}, \tag{17}$$

where $E[\,]$ denotes the expectation value and the constant $S_f\omega_1/k_1$ is introduced to ensure that E_k is dimensionless. The mean squared value of the velocity of the primary mass, m_1, can be written as:

$$E[|\dot{x}_1(t)|^2] = \frac{S_f\omega_1}{m_1 k_1}\int_{-\infty}^{+\infty} |\Gamma(\mathrm{j}\lambda)|^2 \mathrm{d}\lambda. \tag{18}$$

Thus substituting Eq. (9) in (18) and then in (17) yields:

$$E_k = \frac{1}{2}\int_{-\infty}^{+\infty} \left| \frac{B_0+(\mathrm{j}\lambda)B_1+(\mathrm{j}\lambda)^2B_2+(\mathrm{j}\lambda)^3B_3}{A_0+(\mathrm{j}\lambda)A_1+(\mathrm{j}\lambda)^2A_2+(\mathrm{j}\lambda)^3A_3+(\mathrm{j}\lambda)^4A_4} \right|^2 \mathrm{d}\lambda. \tag{19}$$

Eq. (19) can be integrated using the formula in reference [46] leading to:

$$E_k = \frac{1}{2}\frac{G_1\alpha+G_0}{F_2\alpha^2+F_1\alpha+F_0} \tag{20}$$

where the coefficients $G_{0,1}$ and $F_{0,1,2}$ are given in Table A.1 in Appendix A. The optimal control gain α^{opt} that minimise the kinetic energy of the primary system can be calculated by setting to zero the derivative of E_k with respect to α leading to:

$$F_2G_1\alpha^2 + 2F_2G_0\alpha + F_1G_0 - F_0G_1 = 0. \tag{21}$$

As shown in references [43,44,47] a convenient way to tune the control gain is by maximise the power absorbed by the control unit. The total power absorbed by the control unit is given by the sum of the passive power dissipated by the damper and the active power of the electromechanical transducer. The PSD of the power absorbed by the passive damper c_2 is equal to:

$$P_{\mathrm{pas}}(\omega) = \frac{1}{2}\mathrm{Re}\{f_d^*(\mathrm{j}\omega)[\dot{x}_1(\mathrm{j}\omega)-\dot{x}_2(\mathrm{j}\omega)]\}, \tag{22}$$

where * denotes complex conjugate and the force f_d is the force produced by the damper given by:

$$f_d(\mathrm{j}\omega) = c_2(\dot{x}_1(\mathrm{j}\omega)-\dot{x}_2(\mathrm{j}\omega)). \tag{23}$$

Substituting Eq. (23) in (22) the power passively dissipated by the inertial actuator becomes:

$$P_{\mathrm{pas}}(\omega) = \frac{1}{2}c_2|\dot{x}_1(\mathrm{j}\omega)-\dot{x}_2(\mathrm{j}\omega)|^2, \tag{24}$$

The non-dimensional power dissipated by the damper per unit excitation force is given by:

$$I_{\mathrm{pas}} = \frac{c_2 E\left[|\dot{x}_1(t)-\dot{x}_2(t)|^2\right]}{4\pi S_f\omega_1/k_1}, \tag{25}$$

which represents the ratio of the power passively dissipated by the control unit to that generated by the excitation force with spectrum density S_f acting on a damper of value $k_1/(\pi\omega_1)$. The mean squared value of the relative velocity is given by:

$$E[|\dot{x}_1(t)-\dot{x}_2(t)|^2] = \frac{S_f\omega_1^2}{k_1}2\zeta_2\mu\nu\int_{-\infty}^{+\infty} |\Gamma(\mathrm{j}\lambda)-\Theta(\mathrm{j}\lambda)|^2 \mathrm{d}\omega. \tag{26}$$

Please cite this article as: M. Zilletti, Feedback control unit with an inerter proof-mass electrodynamic actuator, *Journal of Sound and Vibration* (2016), http://dx.doi.org/10.1016/j.jsv.2016.01.035

Substituting Eqs. (9) and (10) in Eq. (26) and then in (25) the power passively dissipated by the damper becomes:

$$I_{\text{pas}} = \frac{\zeta_2 \mu \nu}{2\pi} \int_{-\infty}^{+\infty} \left| \frac{D_0 + (\mathrm{j}\lambda) D_1 + (\mathrm{j}\lambda)^2 D_2 + (\mathrm{j}\lambda)^3 D_3}{A_0 + (\mathrm{j}\lambda) A_1 + (\mathrm{j}\lambda)^2 A_2 + (\mathrm{j}\lambda)^3 A_3 + (\mathrm{j}\lambda)^4 A_4} \right|^2 \mathrm{d}\omega, \tag{27}$$

where

$$\begin{aligned} D_0 &= C_0 - B_0 = 0 \\ D_1 &= C_1 - B_1 = 0 \\ D_2 &= C_2 - B_2 = 4\alpha\nu\zeta_2 \\ D_3 &= C_3 - B_3 = -1 \end{aligned} \tag{28}$$

The integral over the frequency band between $\pm\infty$ in Eq. (27) can be calculated using the expression given in reference [46], leading to:

$$I_{\text{pas}} = \frac{1}{2} \frac{H_2 \alpha^2 + H_1 \alpha + H_0}{F_2 \alpha^2 + F_1 \alpha + F_0}, \tag{29}$$

where the coefficients $H_{0,1,2}$ are given in Table A.1 in Appendix A.

The PSD of the active power produced by the electromechanical reactive force is equal to:

$$P_{\text{act}}(\omega) = \frac{1}{2} \mathrm{Re}\{ f_a^*(\mathrm{j}\omega) [\dot{x}^1(\mathrm{j}\omega) - \dot{x}^2(\mathrm{j}\omega)] \}. \tag{30}$$

Assuming that the force f_a is proportional to the velocity $\dot{x}_1(\mathrm{j}\omega)$ of the primary mass, Eq. (30) can be written as:

$$P_{\text{act}}(\omega) = -\frac{g}{2} \mathrm{Re}\{ \dot{x}_1^*(\mathrm{j}\lambda) [\dot{x}_1(\mathrm{j}\omega) - \dot{x}_2(\mathrm{j}\omega)] \} = -\frac{g}{2} \left[|\dot{x}_1(\mathrm{j}\omega)|^2 - \mathrm{Re}\{ \dot{x}_1^*(\mathrm{j}\omega) \dot{x}_2(\mathrm{j}\omega) \} \right]. \tag{31}$$

After some manipulations Eq. (31) can be written as:

$$P_{\text{act}}(\omega) = -\frac{g}{4} \left[|\dot{x}_1(\mathrm{j}\omega)|^2 + |\dot{x}_1(\mathrm{j}\omega) - \dot{x}_2(\mathrm{j}\omega)|^2 - |\dot{x}_2(\mathrm{j}\omega)|^2 \right]. \tag{32}$$

In this case the active power per unit excitation force is given by:

$$I_{\text{act}} = -\frac{gE[|\dot{x}_1(t)|^2 + |\dot{x}_1(t) - \dot{x}_2(t)|^2 - |\dot{x}_2(t)|^2]}{4\pi S_f \omega_1 / k_1}, \tag{33}$$

which represents the ratio of the power actively dissipated by the control unit to that generated by the excitation force with spectrum density S_f acting on a damper of value $k_1/(\pi\omega_1)$. The mean squared value of the relative velocity times the control gain g can be expressed as follow:

$$\begin{aligned} & gE\left[|\dot{x}_1(t)|^2 + |\dot{x}_1(t) - \dot{x}_2(t)|^2 - |\dot{x}_2(t)|^2 \right] \\ &= \frac{S_f \omega_1^2}{k_1} 2\zeta_2 \mu\nu \left[\int_{-\infty}^{+\infty} |\Gamma|^2 \mathrm{d}\lambda + \int_{-\infty}^{+\infty} |\Gamma - \Theta|^2 \mathrm{d}\lambda - \int_{-\infty}^{+\infty} |\Theta|^2 \mathrm{d}\lambda \right] \end{aligned} \tag{34}$$

Substituting the expressions of Γ and Θ in Eq. (34) and calculating the integrals over the frequency band between $\pm\infty$ using the expression given in reference [46] the total active power becomes:

$$I_{\text{act}} = \frac{L_2 \alpha^2 + L_1 \alpha}{F_2 \alpha^2 + F_1 \alpha + F_0}, \tag{35}$$

where the coefficients $L_{1,2}$ are given in Table A.1 in Appendix A. The total power absorbed by the control unit, given by the sum of power dissipated by the passive damper I_{pas} and the active power produced by the electromechanical actuator I_{act} can be written as:

$$I_p = \frac{1}{2} \frac{(2L_2 + H_2)\alpha^2 + (2L_1 + H_1)\alpha + H_0}{F_2 \alpha^2 + F_1 \alpha + F_0}. \tag{36}$$

From the energy balance, in steady state conditions, the total power input into the whole system I_{pin} is equal to the power dissipated by damper 1 plus the total power dissipated by the control unit I_p. The power dissipated by damper 1 is given by:

$$P_1(\omega) = \frac{1}{2} c_1 |\dot{x}_1(\mathrm{j}\omega)|^2. \tag{37}$$

In order to obtain a dimensionless formulation, a dimensionless index relative to $P_1(\omega)$ can be defined by:

$$I_{p1} = \frac{c_1 E\,[|\dot{x}_1(t)|^2]}{4\pi S_f \omega_1^2 / k_1} = \frac{1}{2} \frac{c_1}{m_1} E_k. \tag{38}$$

Please cite this article as: M. Zilletti, Feedback control unit with an inerter proof-mass electrodynamic actuator, *Journal of Sound and Vibration* (2016), http://dx.doi.org/10.1016/j.jsv.2016.01.035

The power input into the system per unit input force can be calculated as the sum of Eqs. (36) and (38) giving:

$$I_{\text{pin}} = I_{p1} + I_p = \frac{1+\delta}{2+2\delta+2\delta\mu}. \tag{39}$$

Eq. (39) indicates that, when the system is excited by a random white noise force, the power input into the system only depends on the masses, m_1 and m_2 and the inertance b_2. Multiplying Eq. (39) by the constant $2\pi S_f \omega_1^2/k_1$ and setting the inertance δ to zero, the power input reduces to $1/(2m_1)$ thus it only depends on the mass of the primary system as shown in references [11,48].

Taking the derivative with respect to α of Eq. (39) yields:

$$\frac{\partial I_{p1}}{\partial \alpha} + \frac{\partial I_p}{\partial \alpha} = 0 \tag{40}$$

and substituting Eq. (38) in (40) gives:

$$\frac{\partial I_p}{\partial \alpha} = -\frac{1}{2}\frac{c_1}{m_1}\frac{\partial E_k}{\partial \alpha}. \tag{41}$$

Eq. (41) indicates that, for given c_1 and m_1, the derivative with respect to α of I_p is proportional to the derivative of E_k thus the maximisation of the power absorbed by the control unit is equivalent to the minimisation of the kinetic energy of the structure under control.

4. Numerical simulations

This section discusses the stability and performance of the velocity feedback loop implemented to control the resonant response of a structure modelled as single degree-of-freedom lumped parameter model.

To better understand the dynamics of the system and compare the vibration control effect obtained with the control unit with and without the inerter numerical simulations have been carried out using the parameters listed in Table 2.

4.1. Stability

The stability of the control system is first assessed with the Nyquist criterion. Fig. 4 shows the Bode (a) and the Nyquist (b) diagrams of the open loop frequency response function (OL-FRF) given by Eq. (13). The dashed line shows the OL-FRF for the classical inertial actuator without the inerter while the solid line shows the OL-FRF of the inertial actuator with the inerter proposed in this study. In order to obtain a non-dimensional formulation the damping ratio of the control unit ζ_2 was defined in Eq. (11) to be independent from the inertance b. However the actual damping ratio of the control unit is indeed influenced by the presence of the inerter thus the actual damping ratio of the inertial actuator ζ_2' is defined as:

$$\zeta_2' = \frac{c_2}{2\sqrt{k_2(m_2+b_2)}}, \tag{42}$$

In order to compare the two configurations the value of the actual damping ratio ζ_2' of the two devices with and without the inerter has been set to 0.1. The OL-FRF in Fig. 4 has been normalised with respect to the magnitude at the second resonance peak in the OL-FRF of the classical configuration without the inerter, so that the differences between the two FRFs can be better compared.

Considering first the classical configuration without the inerter (dashed line) the magnitude of the OL-FRF shows two peaks at about the actuator fundamental resonance frequency ($\lambda = 0.5$) and the fundamental resonance frequency of the system under control ($\lambda = 1$). The two resonant responses are out of phase, thus the low frequency portion of the OL-FRF locus shown in Fig. 4(b) is characterised by a circle in the real-negative quadrants (first resonance) and a circle of larger size in the real-positive quadrants (second resonance). This indicates that the closed feedback loop is only conditionally stable with relatively low gain margin. Considering the case of the control unit with the inerter (solid line) the first peak of the OL-FRF is shifted at about $\lambda = 0.3$ due to the effect of the inerter. The solid line in Fig. 4(b) shows that the circle of the first resonance in the real-negative quadrants is about three times smaller than the one of the classical configuration without the inerter thus it has a gain margin about three times bigger than the classical control unit.

Table 2
Non-dimensional parameters used in the simulations.

Parameter	Value
Mass ratio μ	0.1
Natural frequency ratio ν	0.5
Damping ratio of the primary system ζ_1	0.01
Inertance δ	2
Damping ratio of the inertial actuator ζ_2'	0.1

Please cite this article as: M. Zilletti, Feedback control unit with an inerter proof-mass electrodynamic actuator, *Journal of Sound and Vibration* (2016), http://dx.doi.org/10.1016/j.jsv.2016.01.035

Fig. 5 shows the maximum stable gain of the feedback loop obtained from Eq. (14) as a function of the damping ratio of the inertial actuator ζ_2' and the inerter coefficient δ. The graph shows that the maximum stable gain increases as both the damping ratio and inerter coefficient increase. The use of an inerter in this application is particularly appealing in the light of the fact that a relatively large inertance can be achieved with a small increase of the total mass of the control unit [49].

4.2. Performance

The performance of the controller is assessed in terms of the reduction of the kinetic energy of the system under control when excited by a broadband white noise force. The solid line in Fig. 6 shows the PSD of the kinetic energy of the primary system when the feedback gain, α, is zero.

Since the mass of the actuator is only 10% the mass of the primary system the spectrum of the kinetic energy is dominated by the resonant response of the primary system and the passive effect of the actuator is negligible.

As shown by the dashed line in Fig. 6, as the feedback gain is increased, significant attenuation is initially obtained at resonance frequency of the primary system for both configurations without (a) and with (b) the inerter.

At gains approaching the stability limit (dotted line), however, there is also a significant enhancement of the vibration at the natural frequency of the actuator, due to the positive feedback in this frequency region caused by the phase response of the actuator. Comparing Fig. 6(a) and (b) it can be noticed that for the control unit with the inerter the resonance of the

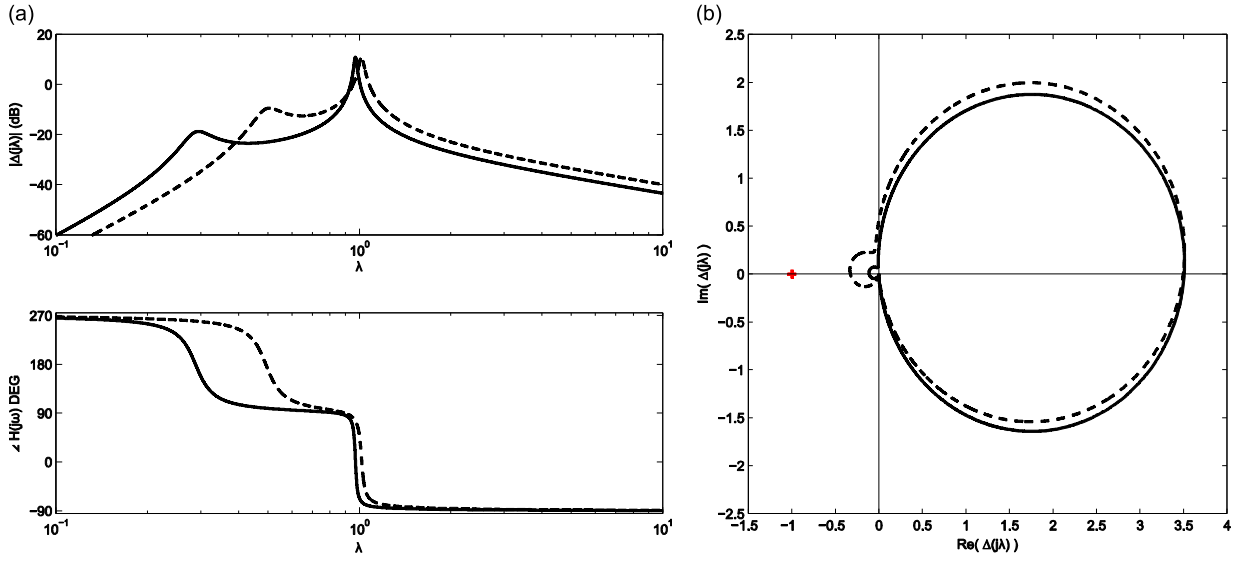

Fig. 4. (a) Bode and (b) Nyquist diagrams of the open loop FRF given in Eq. (13) when $\delta = 0$ (dashed line) and $\delta = 2$ (solid line) for the same value of $\zeta_2' = 0.1$ and normalised to have the same maximum magnitude.

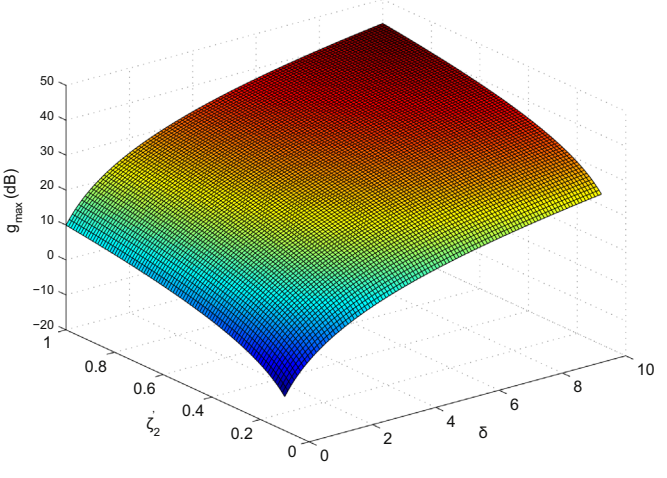

Fig. 5. Maximum stable gain as a function of the damping ratio ζ_2' and the inerter coefficient δ.

Please cite this article as: M. Zilletti, Feedback control unit with an inerter proof-mass electrodynamic actuator, *Journal of Sound and Vibration* (2016), http://dx.doi.org/10.1016/j.jsv.2016.01.035

actuator is shifted down in frequency thus, as shown in the previous subsection, the control system exhibits a greater gain margin which improves the control performance allowing a greater reduction in the spectrum of the kinetic energy of the primary system.

If the total kinetic energy of the primary system is calculated from Eq. (20) its variation with feedback gain, normalised by the kinetic energy with no control, is shown in Fig. 7 for the case with (solid line) and without (dashed line) the inerter. The feedback gain in Fig. 7 has been normalised to the value of maximum stable gain. The total kinetic energy initially decreases as the feedback gain is increased, before increasing again as the maximum stable gain is approached. The minimum of the kinetic energy is reached when the feedback gain is set to the optimal value given by Eq. (21) and is shown by the circular markers. From the plot in Fig. 7 it can be clearly seen that when the inerter is added in parallel with the suspension of the inertial actuator additional 5 dB reduction in the kinetic energy of the primary system can be achieved compare to the case without the inerter when the gain is set to the optimal value.

To better understand the influence of the inerter on the performance of the control unit, the additional reduction in the kinetic energy of the primary system due to the effect of the inerter when the gain is set to the optimal value has been plotted against the inertance δ in Fig. 8.

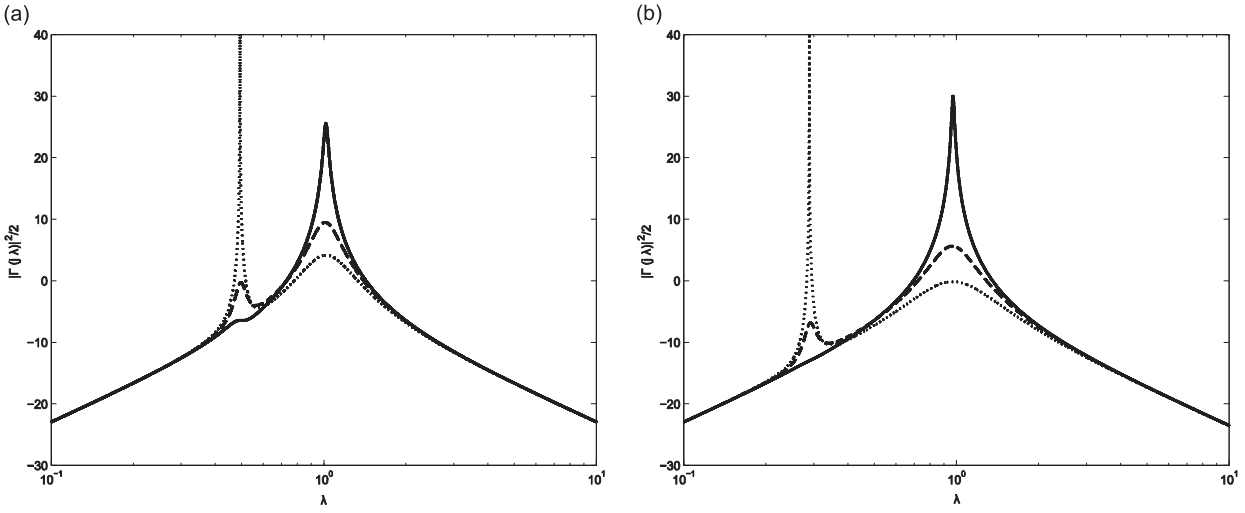

Fig. 6. PSD of the kinetic energy for zero gain (solid line) when the control gain that guarantees 6 dB gain margin (dashed line) and the maximum stable gain (dotted line) are implemented. Inertial actuator (a) without and (b) with the inerter $\delta = 2$.

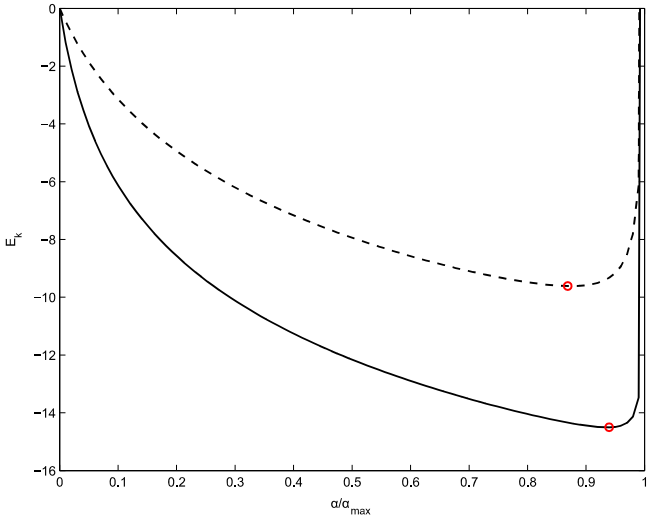

Fig. 7. Reduction in dB of the kinetic energy of the primary system as a function of the control gain g normalised to the maximum stable gain for the control unit with the inerter $b_2 = 0.2$ kg (solid line) and without (dashed line) inerter.

Please cite this article as: M. Zilletti, Feedback control unit with an inerter proof-mass electrodynamic actuator, *Journal of Sound and Vibration* (2016), http://dx.doi.org/10.1016/j.jsv.2016.01.035

The plot shows that a rapid increase in the performance of the control system can be achieved for relatively low values of the inertance δ while for values greater than 20 only a moderate improvement in the performance can be obtained. The circular marker in Fig. 8 shows the value of δ considered the simulations.

As already pointed out in the previous section an alternative control strategy to tune the gain α is to maximise the power absorbed by the controller. Fig. 9 shows the power absorbed by the control unit, I_p, as a function of the normalised feedback gain for the configuration with (solid line) and without (dashed line) the inerter. Fig. 9 shows that when the control gain is zero some power is absorbed by the passive damper of the suspension. As the control gain is increased more and more power is absorbed until a maximum is reached. Comparing the solid and dashed line in Fig. 9 it can be seen that the control unit with the inerter is able to absorb more power than the classical configuration without the inerter. As also analytically demonstrated in the previous section, comparing Figs. 7 and 9 it can be notice that maximising the absorbed power results in the same control gain as minimising the kinetic energy. The control unit could thus be made self-tuneable if an algorithm that adjusts the control gain to maximise the absorbed power is employed [43].

When the control gain approaches the maximum stable value the active force injects power into the system that is then dissipated by the passive damper c_2. This phenomenon becomes more evident when the ratio between m_2 and m_1 decreases. Further investigation on the power flows in the system is currently under investigation.

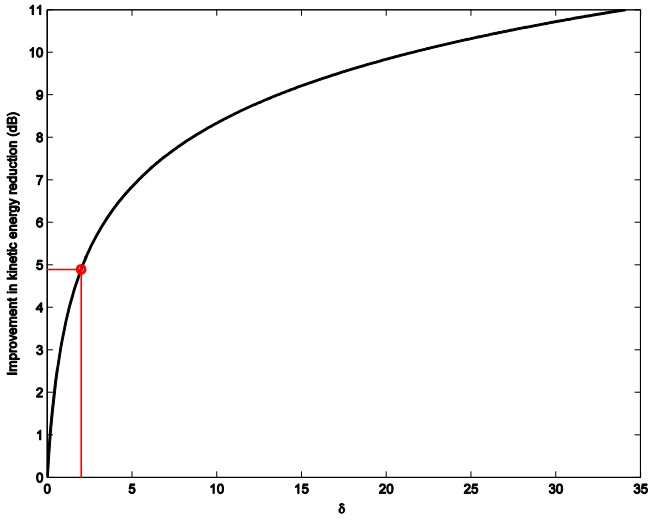

Fig. 8. Improvement in the kinetic energy reduction as a function of δ. The circular marker shows the value of δ considered the simulations.

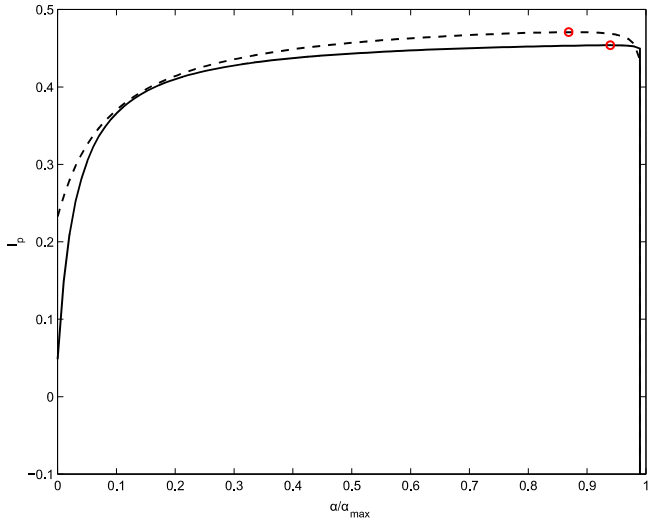

Fig. 9. The power absorbed by the control unit as a function of the control gain g normalised to the maximum stable gain for the control unit with the inerter $b_2 = 0.1$ kg (solid line) and without (dashed line) inerter. The two circular markers show the locations of the maxima.

Please cite this article as: M. Zilletti, Feedback control unit with an inerter proof-mass electrodynamic actuator, *Journal of Sound and Vibration* (2016), http://dx.doi.org/10.1016/j.jsv.2016.01.035

5. Conclusions

This paper presents a theoretical study on the implementation of a velocity feedback loop to reduce the vibration of a structure modelled as a single degree of freedom system. The control unit consist of an inertial actuator with a mass suspended on a spring, a damper and an inerter with an electromechanical transducer in parallel with the suspension. The actuator is fed with a signal proportional to the velocity measured by a sensor located at the footprint of the control unit. It is shown that the use of the inerter has the effect of shifting down the fundamental resonance frequency of the control unit. This allows the use of a relatively stiff spring suspension able to support the static load of the inertial mass and at the same time improve stability and performance of the control system. The study also consider the tuning of the feedback control gain in order to either minimise the kinetic energy of the system under control or maximise the power absorbed by the controller. It has been analytically demonstrated that the two tuning strategies are equivalent.

Acknowledgements

This work was supported by the EPSRC through "Engineering Nonlinearity Project" programme grant (EP/K003836/1).

Appendix A

See Table A.1.

Table A.1
List of coefficients of Eqs. (20), (29) and (35).

$$G_0 = 2\nu\Big(-(1+\delta)^2(1+\mu)\nu^3\zeta_1-(1+\delta)(1+\delta+\delta\mu)\nu^3\zeta_1-(1+\delta)^2\zeta_2-\delta(1+\delta)^2\zeta_2-(1+\delta\quad+\delta\mu)\nu^4\zeta_2-\mu(1+\delta+\delta\mu)\nu^4\zeta_2-4(1+\delta)^2\nu^2\zeta_1^2\zeta_2-4(1+\delta)^2\nu\zeta_1\zeta_2^2 \\ +2(1+\delta\quad+\delta\mu)\nu^2(\nu\zeta_1+\zeta_2)(1+\delta-2\zeta_2^2)\Big)$$

$$G_1 = 4\mu\nu^3((1+\delta)^2-(1+\delta+\delta\mu)\nu^2)\zeta_2$$

$$F_0 = 4(1+\delta+\delta\mu)\nu\big(-4(1+\delta)\nu^2\zeta_1^3\zeta_2-\mu\nu\zeta_2^2-\zeta_1\zeta_2\big(1+\delta^2-2\nu^2+\nu^4+2\mu\nu^4+\mu^2\nu^4-2\delta\big(-1+(1\quad+\mu)\nu^2\big)+4(1+\mu)\nu^2\zeta_2^2\big)-\nu\zeta_1^2\big(\mu\nu^2+4\big(1+\delta+(1+\mu)\nu^2\big)\zeta_2^2\big)\big)$$

$$F_1 = 8\mu(1+\delta+\delta\mu)\nu^2\zeta_2(2(1+\delta)\nu\zeta_1+2\nu^2\zeta_2+2\mu\nu^2\zeta_2-(\nu\zeta_1+\zeta_2)(1+\delta+\nu^2+\mu\nu^2+4\nu\zeta_1\zeta_2))$$

$$F_2 = 16\mu^2(1+\delta+\delta\mu)\nu^4\zeta_2^2$$

$$H_0 = -\mu\nu\zeta_2((1+\delta)\zeta_2+4\nu^2\zeta_1^2\zeta_2+\zeta_1((1+\mu)\nu^3+4\nu\zeta_2^2))$$

$$H_1 = 2\mu^2\nu^3\zeta_2^2$$

$$H_2 = -16\mu(1+\delta+\delta\mu)\nu^3\zeta_2^3(\nu\zeta_1+\zeta_2)$$

$$L_1 = \mu\nu\zeta_2((1+\delta^2-\nu^2-\delta(-2+(1+\mu)\nu^2))\zeta_2+4(1+\delta)\nu^2\zeta_1^2\zeta_2+\nu\zeta_1(\mu\nu^2+4(1+\delta)\zeta_2^2))$$

$$L_2 = 2\mu\nu^3\zeta_2^2(-(1+\delta)\mu-4(1+\delta+\delta\mu)\nu\zeta_1\zeta_2-4(1+\delta+\delta\mu)\zeta_2^2)$$

References

[1] H. Frahm, *Device for damping vibrations of bodies*, U.S. Patent, 989,958, 1911.
[2] J.P. Den Hartog, *Mechanical Vibrations*, 4th ed. McGraw-Hill, New York, 1956.
[3] T. Asami, O. Nishihara, A.M. Baz, Analytical solutions to H∞ and H2 optimization of dynamic vibration absorbers attached to damped linear systems, *Journal of Vibration and Acoustics* 124 (2002) 284–295.
[4] S.H. Crandall, W.D. Mark, *Random Vibration in Mechanical Systems*, Academic Press, New York, 1963.
[5] Y. Iwata, On the construction of the dynamic vibration absorber, *Japanese Society of Mechanical Engineering* 820 (1982) 150–152.
[6] S. Krenk, Frequency analysis of the tuned mass damper, *Journal of Applied Mechanics* 72 (2005) 936–942.
[7] O. Nishihara, T. Asami, Closed-form solutions to the exact optimizations of dynamic vibration absorbers (minimizations of the maximum amplitude magnification factors), *Journal of Vibration and Acoustics* 124 (2002) 576–582.
[8] O. Nishihara, H. Matsuhisa, Design of a dynamic vibration absorber for minimisation of maximum amplitude magnification factor (derivation of algebric exact solution), *Transactions of the Japan Society of Mechanical Engineers, Series C* 62–614 (1997) 3438–3445.
[9] G.B. Warburton, Optimum absorber parameters for various combinations of response and excitation parameters, *Journal of Earthquake Engineering and Structural Dynamics* 10 (1982) 381–401.
[10] H. Yamaguchi, Damping of transient vibration by a dynamic absorber, *Transactions of the Japan Society of Mechanical Engineers, Series C* 54 (1988) 561–568.
[11] M. Zilletti, S.J. Elliott, E. Rustighi, Optimisation of dynamic vibration absorbers to minimise kinetic energy and maximise internal power dissipation, *Journal of Sound and Vibration* 331 (2012) 4093–4100.
[12] L. Zuo, S.A. Nayfeh, Minimax optimization of multi-degree-of-freedom tuned-mass dampers, *Journal of Sound and Vibration* 272 (2004) 893–908.
[13] P. Gardonio, M. Zilletti, Integrated tuned vibration absorbers: a theoretical study, *The Journal of the Acoustical Society of America* 134 (2013) 3631–3644.
[14] P. Gardonio, M. Zilletti, Sweeping tuneable vibration absorbers for low-mid frequencies vibration control, *Journal of Sound and Vibration* 354 (2015) 1–12.

Please cite this article as: M. Zilletti, Feedback control unit with an inerter proof-mass electrodynamic actuator, *Journal of Sound and Vibration* (2016), http://dx.doi.org/10.1016/j.jsv.2016.01.035

[15] M. Zilletti, P. Gardonio, Experimental implementation of switching and sweeping tuneable vibration absorbers for broadband vibration control, *Journal of Sound and Vibration* 334 (2015) 164–177.
[16] F. Fahy, P. Gardonio, *Sound and Structural Vibration, Radiation, Transmission and Response*, 2nd ed. Academic Press, Oxford, UK, 2007.
[17] S.J. Elliott, Global vibration control through local feedback, in: D. Wagg, I. Bond, P. Weaver, M. Friswell (Eds.), *Adaptive Structure: Engineering Applications*, John Wiley & Sons Ltd., Chichester2007, pp. 59–87.
[18] S.J. Elliott, P. Gardonio, T.C. Sors, M.J. Brennan, Active vibroacoustic control with multiple local feedback loops, *The Journal of the Acoustical Society of America* 111 (2002) 908–915.
[19] C. González Díaz, P. Gardonio, Feedback control laws for proof-mass electrodynamic actuators, *Smart Materials and Structures* 16 (2007) 1766.
[20] A. Preumont, *Vibration Control of Active Structures*, Kluwer Academic, London, 2002.
[21] S.J. Elliott, M. Serrand, P. Gardonio, Feedback stability limits for active isolation systems with reactive and inertial actuators, *Transactions of the ASME, Journal of Vibration and Acoustics* 123 (2001) 250–261.
[22] L. Benassi, S.J. Elliott, Active vibration isolation using an inertial actuator with local displacement feedback control, *Journal of Sound and Vibration* 278 (2004) 705–724.
[23] C. Paulitsch, P. Gardonio, S.J. Elliott, Active vibration control using an inertial actuator with internal damping, *The Journal of the Acoustical Society of America* 119 (2006) 2131–2140.
[24] J. Rohlfing, S.J. Elliott, P. Gardonio, Feedback compensator for control units with proof-mass electrodynamic actuators, *Journal of Sound and Vibration* 331 (2012) 3437–3450.
[25] M.C. Smith, Synthesis of mechanical networks: the inerter, *IEEE Transactions on Automatic Control* 47 (2002) 1648–1662.
[26] Y. Hu, M.Z.Q. Chen, Performance evaluation for inerter-based dynamic vibration absorbers, *International Journal of Mechanical Sciences* 99 (2015) 297–307.
[27] P. Brzeski, E. Pavlovskaia, T. Kapitaniak, P. Perlikowski, The application of inerter in tuned mass absorber, *International Journal of Non-Linear Mechanics* 70 (2015) 20–29.
[28] P. Brzeski, T. Kapitaniak, P. Perlikowski, Novel type of tuned mass damper with inerter which enables changes of inertance, *Journal of Sound and Vibration* 349 (2015) 56–66.
[29] M.C. Smith, F.-C. Wang, Performance benefits in passive vehicle suspensions employing inerters, *Vehicle System Dynamics* 42 (2004) 235–257.
[30] M.Z.Q. Chen, C. Papageorgiou, F. Scheibe, W. Fu-cheng, M.C. Smith, The missing mechanical circuit element, *IEEE Circuits and Systems Magazine* 9 (2009) 10–26.
[31] Y. Shen, L. Chen, X. Yang, D. Shi, J. Yang, Improved design of dynamic vibration absorber by using the inerter and its application in vehicle suspension, *Journal of Sound and Vibration* 361 (2016) 148–158.
[32] P. Li, J. Lam, K.C. Cheung, Control of vehicle suspension using an adaptive inerter, *Proceedings of the Institution of Mechanical Engineers, Part D: Journal of Automobile Engineering* (2015).
[33] M.Z.Q. Chen, K. Wang, S. Zhan, L. Chanying, Realizations of a special class of admittances with strictly lower complexity than canonical forms, *IEEE Transactions on Circuits and Systems I: Regular Papers* 60 (2013) 2465–2473.
[34] M.Z.Q. Chen, K. Wang, Y. Zou, J. Lam, Realization of a special class of admittances with one damper and one inerter for mechanical control, *IEEE Transactions on Automatic Control* 58 (2013) 1841–1846.
[35] K. Wang, M.Z.Q. Chen, Y. Hu, Synthesis of biquadratic impedances with at most four passive elements, *Journal of the Franklin Institute* 351 (2014) 1251–1267.
[36] S. Evangelou, D.J.N. Limebeer, R.S. Sharp, M.C. Smith, Control of motorcycle steering instabilities, *IEEE Control Systems* 26 (2006) 78–88.
[37] S. Evangelou, D.J.N. Limebeer, R.S. Sharp, M.C. Smith, Mechanical steering compensators for high-performance motorcycles, *Journal of Applied Mechanics* 74 (2006) 332–346.
[38] F.-C. Wang, M.-K. Liao, B.-H. Liao, W.-J. Su, H.-A. Chan, The performance improvements of train suspension systems with mechanical networks employing inerters, *Vehicle System Dynamics* 47 (2009) 805–830.
[39] J.Z. Jiang, A.Z. Matamoros-Sanchez, R.M. Goodall, M.C. Smith, Passive suspensions incorporating inerters for railway vehicles, *Vehicle System Dynamics* 50 (2012) 263–276.
[40] F.-C. Wang, M.-F. Hong, C.-W. Chen, Building suspensions with inerters, *Proceedings of the Institution of Mechanical Engineers, Part C: Journal of Mechanical Engineering Science* 224 (2010) 1605–1616.
[41] X. Dong, Y. Liu, M.Z.Q. Chen, Application of inerter to aircraft landing gear suspension, *Proceedings of the 34th Chinese Control Conference (CCC)*, 2015, pp. 2066–2071.
[42] M.Z.Q. Chen, Y. Hu, L. Huang, G. Chen, Influence of inerter on natural frequencies of vibration systems, *Journal of Sound and Vibration* 333 (2014) 1874–1887.
[43] M. Zilletti, S.J. Elliott, P. Gardonio, Self-tuning control systems of decentralised velocity feedback, *Journal of Sound and Vibration* 329 (2010) 2738–2750.
[44] M. Zilletti, S.J. Elliott, P. Gardonio, E. Rustighi, Experimental implementation of a self-tuning control system for decentralised velocity feedback, *Journal of Sound and Vibration* 331 (2012) 1–14.
[45] M. Zilletti, P. Gardonio, S.J. Elliott, Optimisation of a velocity feedback controller to minimise kinetic energy and maximise power dissipation, *Journal of Sound and Vibration* 333 (2014) 4405–4414.
[46] D.E. Newland, *An Introduction to Random Vibrations, Spectral & Wavelet Analysis*, Third edition ed. Dover Publications, Inc., Mineola, New York, 1975.
[47] S.J. Elliott, M. Zilletti, P. Gardonio, *Apparatus and method of vibration control*, Patent, WO2011114165 A1, 2011.
[48] R.S. Langley, A general mass law for broadband energy harvesting, *Journal of Sound and Vibration* 333 (2014) 927–936.
[49] Y. Hu, M.Z.Q. Chen, Z. Shu, L. Huang, Analysis and optimisation for inerter-based isolators via fixed-point theory and algebraic solution, *Journal of Sound and Vibration* 346 (2015) 17–36.

Please cite this article as: M. Zilletti, Feedback control unit with an inerter proof-mass electrodynamic actuator, *Journal of Sound and Vibration* (2016), http://dx.doi.org/10.1016/j.jsv.2016.01.035